

---

# Application of the MST clustering to the high energy $\gamma$ -ray sky.

## I - New possible detection of high-energy $\gamma$ -ray emission associated with BL Lac objects

R. Campana • E. Massaro • E. Bernieri •  
Q. D'Amato

**Abstract** In this paper we show an application of the Minimum Spanning Tree (MST) clustering method to the high-energy  $\gamma$ -ray sky observed at energies higher than 10 GeV in 6.3 years by the *Fermi*-Large Area Telescope. We report the detection of 19 new high-energy  $\gamma$ -ray clusters with good selection parameters whose centroid coordinates were found matching the positions of known BL Lac objects in the 5th Edition of the Roma-BZCAT catalogue. A brief summary of the properties of these sources is presented.

**Keywords** gamma rays: general gamma rays: galaxies: active: BL Lac objects methods: data analysis

### 1 Introduction

Observational  $\gamma$ -ray astronomy in the GeV range is a new window on the universe opened by the *Fermi*-Large Area Telescope (LAT) mission. The number of photons having energies higher than a few GeV collected by this instrument in more than six years since August 2008

is large enough to allow the detection of many Galactic and extragalactic sources. The first catalogue of sources detected above 10 GeV in the first three years of the *Fermi* mission (1FHL, Ackermann et al. 2013b) contains 514 objects, of which 393 are associated with Active Galactic Nuclei (AGNs) with a large dominance of BL Lac objects (259 sources, about 50% of the entire catalogue). A previous catalogue at even higher energies ( $>100$  GeV) was realized by Neronov et al. (2011).

In previous works (Campana et al. 2008, 2013; Bernieri et al. 2013) we adapted a clustering method based on the Minimum Spanning Tree (hereafter MST) topometric algorithm for detecting photon concentrations in LAT  $\gamma$ -ray images of the sky, and developed some useful indicators to select clusters having a significance high enough to be genuine. This method works well in not very dense photon fields with a rather uniform background and has a good performance in extracting weak sources appearing as quite compact clusters of four or five photons. MST was already applied in preparing the 1FHL and the 1FGL (Abdo et al. 2010) and 2FGL (Nolan et al. 2012) catalogues of the *Fermi*-LAT collaboration. Other clustering methods have been applied to  $\gamma$ -ray source searches in the *Fermi*-LAT sky images such that by Neronov et al. (2011), and DBSCAN by Tramacere and Vecchio (2013).

In this paper we show an example of MST application to the high-energy ( $>10$  GeV) *Fermi*-LAT sky. Several new rather faint clusters were found very close to the position of known BL Lac objects reported in the 5th Edition of the Multifrequency Blazar Catalogue Roma-BZCAT (Massaro et al. 2014, 2015, hereafter 5BZCAT) and having all the characteristics of genuine  $\gamma$ -ray emitters. In the following Sections we describe the main properties of these sources which are interesting to bridge GeV and TeV astronomy.

---

R. Campana

INAF-IASF-Bologna, via Piero Gobetti 101, I-40129, Bologna, Italy

E. Massaro

INAF-IAPS, via del Fosso del Cavaliere 100, I-00133, Roma, Italy

and

In Unam Sapientiam, Roma, Italy

E. Bernieri

INFN-Sezione di Roma Tre, via della Vasca Navale 84, I-00146 Roma, Italy

Q. D'Amato

Dipartimento di Matematica e Fisica, Università di Roma Tre, via della Vasca Navale 84, I-00146 Roma, Italy

## 2 $\gamma$ -ray source detection by means of the MST algorithm

We first present a short review our method based on MST: for a more complete description see Campana et al. (2008, 2013).

Given a set of  $N$  points (*nodes*) in a 2-dimensional space, we can compute the set  $\{\lambda_i\}$  of weighted *edges* connecting them. For a set of points in a Cartesian frame, the edges are the lines joining the nodes, weighted by their length. The MST is a graph without closed loops (*tree*) connecting all the nodes with the minimum total weight,  $\min[\sum_i \lambda_i]$ .

We divided the LAT sky in several regions to take into account the presence of the Galactic emission and considered the photon arrival directions as nodes in a graph, with the angular distance between them as the edge weight. Once the MST was computed for each region, a set of subtrees corresponding to clusters of photons was extracted by means of the following operations: *i) separation*: by removing all the edges having a length  $\lambda > \Lambda_{\text{cut}}$ , the separation value, a set of disconnected sub-trees is obtained; *ii) elimination*: by removing all the sub-trees having a number of nodes  $n \leq N_{\text{cut}}$  to eliminate very small casual clusters of photons, only the clusters having a size above this threshold are left.

The separation value is usually defined in units of the mean edge length  $\Lambda_m = (\sum_i \lambda_i)/N$  in the MST. The remaining set of sub-trees provides a first list of candidate  $\gamma$ -ray sources and a *secondary* selection must be done to select the most robust candidates, removing the greatest number of spurious/random clusters. Campana et al. (2013) proposed a useful indicator for this selection, the so-called *magnitude* of the cluster, defined as:

$$M_k = n_k g_k \quad (1)$$

where  $n_k$  is the number of nodes in the cluster  $k$  and  $g_k$  is the *clustering parameter*:

$$g_k = \Lambda_m / \lambda_{m,k} \quad (2)$$

that is the ratio between the mean edge length over the entire tree and the mean edge length of the  $k$ -th cluster.

The magnitude  $M$  quantifies the trade-off between the number of photons ( $n$ ) and their “clumpiness” ( $g$ ): a small tree in terms of photons can be highly clustered and therefore significant.  $M$  was shown to be a good parameter for evaluating the “goodness” of the accepted clusters. On the basis of tests performed in simulated and real *Fermi*-LAT fields, Campana et al. (2013) verified that  $\sqrt{M}$  has a high linear correlation

with other statistical significance parameters, derived from a wavelet based algorithm and from maximum likelihood analysis, and that it can be used as a good estimator of statistical significance of MST detections. In particular, threshold values of  $M$  above 15–17 are shown (Campana et al. 2013) to reject the large majority of spurious (low significance) clusters.

Another useful parameter is the *median radius*  $R_m$ , i.e. the radius of the circle centred at the cluster centroid and containing the 50% of photons in the cluster, that for a cluster that can be associated with a genuine pointlike  $\gamma$ -ray source should be smaller than or comparable to the 68% containment radius of the instrumental Point Spread Function (PSF). For *Fermi*-LAT<sup>1</sup>, this radius varies from  $0^\circ:35 \equiv 21'$  at 3 GeV to  $0^\circ:2 \equiv 12'$  at 10 GeV (see also Ackermann et al. 2013a). Moreover, we also expect that the angular distance between the positions of the cluster centroid and the possible optical counterpart are lower than the latter value.

## 3 Detection of $\gamma$ -ray emission associated with BL Lac objects

LAT data (Pass 7 reprocessed v15, event class 2) above 10 GeV, covering the whole sky in the  $\sim 6.3$  years time range from the start of mission (2008 August 04) up to 2014 December 04, were downloaded from the FSSC archive<sup>2</sup>. Standard cuts on the zenith angle ( $100^\circ$ ) and data quality were applied.

The sky far from the Galactic plane ( $|b| \geq 20^\circ$ ) was then divided in several broad regions to take into account the Galactic latitude dependence of the background level and consequently of the S/N ratio. In each region the MST was computed and clusters were obtained using a cut length  $\Lambda_{\text{cut}} = 0.75 \Lambda_m$  and a threshold number  $N_{\text{cut}}$  of 4 photons in a cluster. Then a secondary selection was performed limiting the  $M$  value to be higher than 15. The large majority of selected clusters resulted in a very good positional agreement with the corresponding 3FGL (Acero et al. 2015) and 1FHL sources. As an example, on the explored extra-Galactic sky the 1FHL catalogue reports 268 sources. Within a matching distance equal to the 95% containment radius ( $0^\circ:5 \equiv 30'$ ) from them we found 258 corresponding MST clusters passing the primary selection. Almost all of these clusters ( $\sim 99\%$ ) have a magnitude  $M > 15$ , thus passing also the secondary selection.

<sup>1</sup><http://www.slac.stanford.edu/exp/glast/groups/canda/lat.Performance.htm>

<sup>2</sup><http://fermi.gsfc.nasa.gov/ssc/data/access/>

We also found several clusters not reported as sources in these catalogues. We searched for associations of the unreported clusters with the 5BZCAT (Massaro et al. 2014, 2015), that contains 3561 sources classified as classical BL Lac objects (BZB), galaxy-dominated blazars (BZG), flat-spectrum radio quasars (BZQ) and blazars of uncertain type (BZU). We did not perform any *a priori* selection criteria on the radio flux.<sup>3</sup> The matching radius for the association is  $0.1 \equiv 6'$ , smaller than the PSF radius at the considered energies. This value can be justified looking at Figure 1, that shows the angular separation between the 467 MST cluster centroids that have a correspondence with 3FGL sources within a  $30'$  matching distance, and the safe 5BZCAT counterpart (thus with a very precise optical and radio location) to which the latter ones were associated. The large majority ( $\sim 90\%$ ) of these sources, even for weaker clusters (red histogram in Figure 1, corresponding to clusters with a number of nodes  $n \leq 12$ ) have a separation smaller than  $6'$ .

We found 19 high-energy photon clusters, without any correspondence with the 3FGL and 1FHL catalogues, having thus a position very close to the accurate optical and radio ones of BL Lac objects. Twelve of them have  $M > 18$  and, according to the simulations by Campana et al. (2013) their probability to be spurious, based on this parameter alone, is expected to be lower than 2%.

One must be aware that the finding of a cluster is basically an indication of the presence of a small region in which the photons are denser than in the surroundings, and it does not necessarily correspond to an actual  $\gamma$ -ray source with the expected properties according to the instrumental response. This can be established only by a further analysis that takes into account these properties. In practice, we verified in the entire extragalactic sky ( $|b| > 15^\circ$ ) that all clusters at energies above 10 GeV having  $M > 32$  and about one third of those with  $15 < M < 20$  have a firm 3FGL counterpart.

Under this respect cluster analysis is important for investigating the population of sources with a photon number too low for obtaining a significant matching with the PSF profile.

Figure 2 presents a map of a large sky region illustrating this result: it contains 30  $\gamma$ -ray MST clusters of which 25 are coincident with 3FGL sources (12 also

with 1FHL sources), while 3 of the 5 unassociated clusters match the position of BL Lac objects.

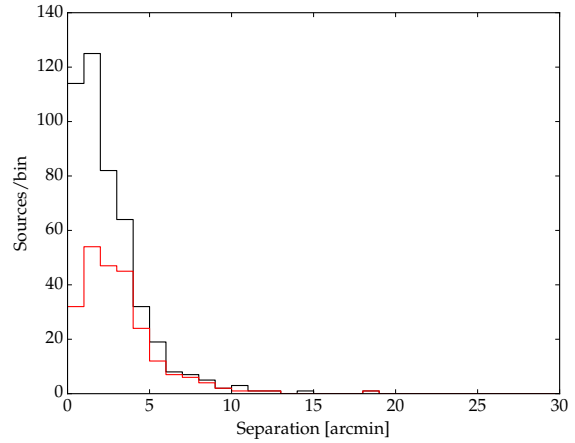


**Fig. 1** Histogram of the angular separation between the locations of the 5BZCAT counterparts of the identified 3FGL sources with respect to the MST cluster centroid. The black line refers to all the clusters, the red line to the clusters having  $n \leq 12$ .

Table 1 lists the main properties of the newly found clusters and their associated BL Lac objects. In this table the coordinates of cluster centroids and the relevant MST parameters are reported, with some astrophysical data, like optical magnitudes, redshift, and the  $\text{Log } \Phi_{\text{XR}}$ , the normalised ratio between the X-ray to the radio flux:

$$\Phi_{\text{XR}} = 10^2 F_X / S_{1.4} \Delta\nu \quad (3)$$

where  $F_X$  is in the band 0.1–2.4 keV in units of  $10^{-12}$  erg  $\text{cm}^{-2}$   $\text{s}^{-1}$  and  $S_{1.4}$  is the radio flux density at 1.4 GHz in mJy with a bandwidth  $\Delta\nu$  of 1 GHz. This dimensionless parameter (Massaro et al. 2012) can be used as a simple indicator if a BL Lac object would be classified HBL (High Energy peaked BL Lacs) or LBL (Low Energy peaked BL Lacs) depending if its decimal logarithm is higher or lower than 0.25.

Note that the median radius  $R_m$  is within the 68% containment PSF radius and that the highest angular separation is  $5.7$ , smaller than the 50% of this radius, confirming the robustness of the spatial association.

Assuming a prevailing uniform random origin of the diffuse background (far from the Galactic plane) the significance of a cluster detection can be estimated by means of the probability to find a cluster having the similar  $N$ ,  $g$  and  $M$  in a large set of randomly distributed photons. We generated 10000 simulated random fields with 50, 125 and 200 points, reflecting the typical number of photons in the 20 different  $6^\circ \times 6^\circ$

<sup>3</sup>The fact that some sources are faint in the radio is typical of HBL objects. The 3LAC catalogue, for instance, includes 48 sources with a radio flux at 1.4 GHz lower than 10 mJy (about all of HSP type). Considering the fact that we are searching for faint gamma-ray sources (the bright ones are already in the 3FGL catalogue!) it is reasonable to assume they could be also faint in the radio band.

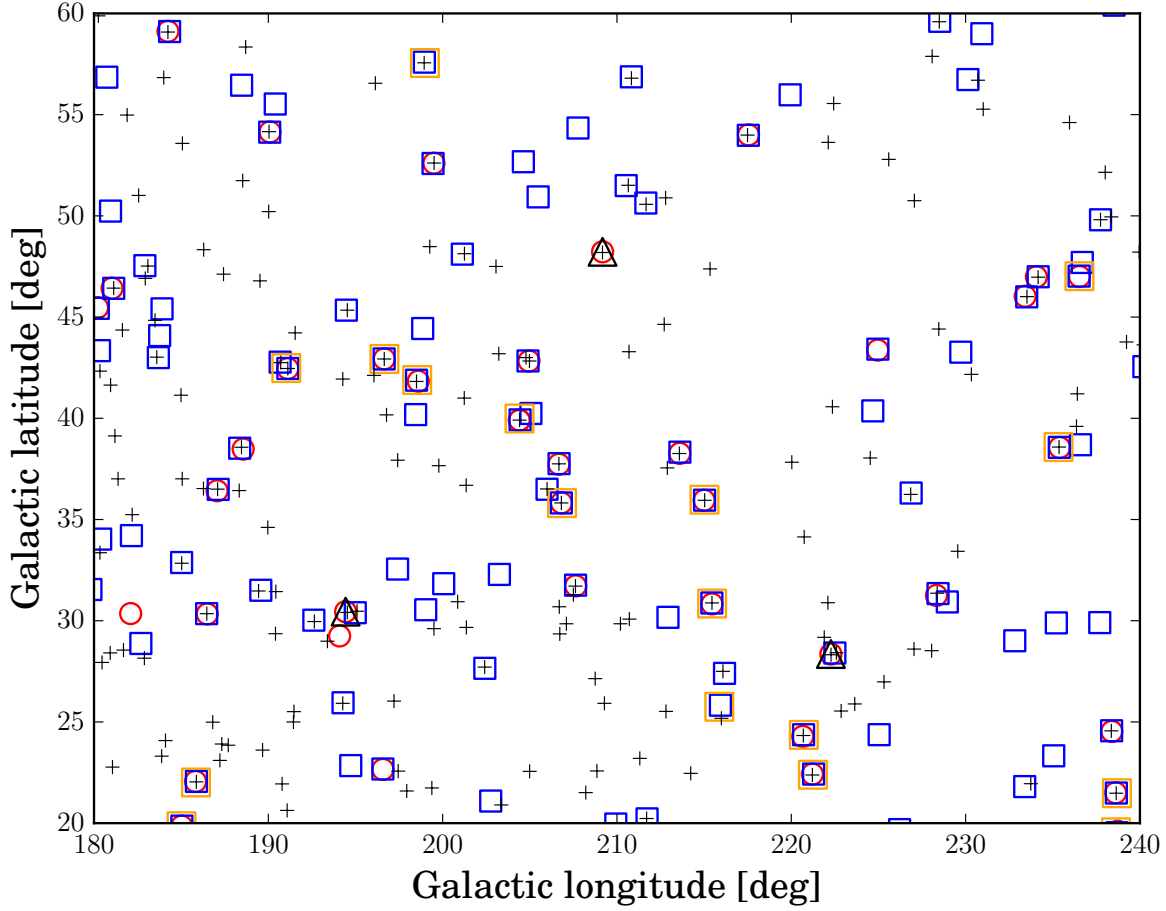


**Fig. 2** A large region of the sky in Galactic coordinates ( $60^\circ \times 40^\circ$ ) showing the MST  $\gamma$ -ray source detections at energies higher than 10 GeV (red circles), superposed to BL Lac objects in the 5th Edition of the Roma-BZCAT (black crosses) and to the 3FGL and 1FHL  $\gamma$ -ray source catalogues (blue and orange squares, respectively). Note the excellent positional agreement between MST and 3FGL counterparts. Two MST clusters are unassociated and three other correspond to BL Lac objects but not to 3FGL catalogue sources (black triangles).

**Table 1** New MST sources observed at  $E > 10$  GeV and their 5BZCAT associations. Columns 2–7 report the MST parameters of the MST cluster. Source data in columns 8–11 are from 5BZCAT. Magnitudes with the r code are from SDSS DR10; the symbols : and :: indicate uncertain and very uncertain data. Column 12 shows the angular separation between the cluster centroid and the 5BZB source. The last column reports the detection significance in equivalent Gaussian standard deviations, see text for details.

MST source	RA J2000	DEC J2000	$n$	$g$	$M$	$R_m$ deg	BZCAT association	$z$	$R$ mag	Log $\Phi_{\text{XR}}$	Sep.	$P$ $\sigma$
MST 0204–3333	31.166	-33.559	5	4.66	23.27	0.09	5BZB J0204–3333	0.617	19.1	1.38	5'7	4.34
MST 0236–2940	39.007	-29.671	9	2.47	22.20	0.16	5BZB J0235–2938	-	19.0	1.50	5'6	5.38
MST 0336–0347	54.095	-3.795	7	2.26	15.81	0.16	5BZB J0336–0347	0.162:	16.3	0.51	0'3	5.48
MST 0801+6442	120.411	64.705	9	3.12	28.10	0.11	5BZB J0801+6444	0.20	18.9	0.75	4'6	5.02
MST 0803+2440	120.766	24.683	6	2.65	15.90	0.14	5BZB J0803+2437	-	18.8r	0.03	3'2	4.42
MST 0818+2819	124.626	28.325	7	3.60	25.19	0.07	5BZB J0818+2814	0.226	17.4	-0.69	5'5	5.00
MST 0848+0503	132.248	5.064	12	3.04	36.47	0.16	5BZB J0848+0506	-	20.2	1.91	5'5	5.02
MST 0932+1042	143.208	10.711	5	4.80	23.99	0.08	5BZB J0932+1042	0.361	18.0r	0.24	2'6	5.10
MST 0947+2215	146.941	22.266	6	3.20	19.22	0.09	5BZB J0947+2215	-	19.1r	-	1'7	5.43
MST 0951+7503	147.913	75.062	6	3.03	18.09	0.08	5BZB J0952+7502	0.179	15.6	1.31	3'3	4.70
MST 1005+6443	151.457	64.723	6	2.53	15.20	0.09	5BZB J1006+6440	-	18.9	0.15	4'0	3.98
MST 1137–1706	174.474	-17.115	5	3.81	19.05	0.06	5BZB J1137–1710	0.600	19.0	1.64	3'8	4.66
MST 1216–0241	184.031	-2.695	5	3.44	17.18	0.06	5BZB J1216–0243	0.359	17.2r	1.02	1'7	4.64
MST 1311+3951	197.924	39.865	6	2.99	17.95	0.09	5BZB J1311+3953	-	19.8r	-0.16	1'6	4.98
MST 1352+5557	208.235	55.956	7	2.27	15.89	0.11	5BZB J1353+5600	0.404	18.4r	1.13	5'7	4.07
MST 1423+1414	215.856	14.237	5	3.29	16.47	0.04	5BZB J1423+1412	0.769::	19.1r	-	1'9	4.70
MST 1423+3736	215.815	37.615	10	2.21	22.10	0.20	5BZB J1423+3737	-	18.5r	-0.62	2'2	5.46
MST 1627+3148	246.780	31.813	7	2.97	20.81	0.05	5BZB J1627+3149	-	19.9r	-	1'7	5.55
MST 2211–0004	332.819	-0.070	7	3.41	23.90	0.09	5BZB J2211–0003	0.362	18.7r	0.79	2'4	5.14

fields used for verifying the detection significance. Assuming that  $N_s$ ,  $g_s$  and  $M_s$  are the values of these parameters for a particular source, the number of random generated clusters with  $N \geq N_s$ ,  $g \geq g_s$  and  $M \geq M_s$ , divided by the total number of random clusters, provides the upper limit to the probability that the source is of spurious origin. Moreover, one has to evaluate the probability that the found cluster is located at a short angular distance from a BL Lac object not already associated with a  $\gamma$ -ray source. Simple estimates for these probabilities can be obtained as the ratio between the solid angle of a circle having the radius equal to the angular separation between the BL Lac objects and the cluster centroids, to the solid angle covered by the  $6^\circ \times 6^\circ$  regions used for verifying the detection significance, eventually multiplied for the number of known BL Lac objects inside the field, with the exclusion of those already associated with known  $\gamma$ -ray sources. These ratios range from  $6.2 \cdot 10^{-5}$  for 5BZB J1311+3953 to  $7.9 \cdot 10^{-4}$  for 5BZB J0204–3333, the source with the largest angular separation. Combining these two independent probabilities we obtain the final significance of a detection, expressed as the probability  $P$  in equivalent Gaussian standard deviations, for a chance coincidence of a spurious cluster with a known BL Lac object (Table 1). For all clusters these combined significances are above  $3.98\sigma$ , while for more than half of them it is in excess of  $5\sigma$ .

Fifteen of the 19 sources reported in Table 1 do not have another 5BZCAT source associated within a  $0.5 \equiv 30'$  radius. For three of the remaining 4 sources, the other possible associations are much weaker than the proposed ones, being sufficiently far away (more than  $15'$  distant). The last source, and some of the other associations between 5BZCAT blazars and MST clusters, will be discussed in the following Section. Regarding the possibility to have a counterpart to these clusters different from a BL Lac object, in general in the same search radius there are only few weak radio sources (e.g. reported by the NVSS<sup>4</sup> and FIRST<sup>5</sup> catalogues) usually without a safe optical counterpart, or for MST 1423+1414 a faint optical (SDSS) quasar undetected in the radio band. Other possible associations as narrow-line Seyfert 1 objects or classified radio galaxies are not found. The association with 5BZCAT objects appears therefore much more robust than for other sources.

To increase the confidence on these detections we performed a MST cluster search in rather small regions centered at the cluster position and having a size of

about  $6^\circ \times 6^\circ$ . All clusters upon consideration were confirmed and they were the only unassociated sources with  $M > 15$ . The only exception was a cluster in the field of MST 1423+3736 at about  $2.4$ . Furthermore, we performed a similar check considering also photon energies higher than 3 GeV and again the candidate selections were found, with similar MST cluster parameters, with the only exception of MST 0951+7503, that was undetected.

We extracted also aperture photometry light curves for all the 19 candidate sources in various energy bands. With the exception of MST 1423+3736 (see Sect. 4.8) there is no evidence of variable activity or flares for the other sources.

### 3.1 Results from likelihood analysis

We performed also a standard unbinned likelihood analysis for each MST cluster. A Region of Interest (ROI) of  $10^\circ$  radius was selected centered at the MST cluster centroid, and standard screening criteria were applied to the *Fermi*-LAT data above 3 GeV. The likelihood analysis was performed considering all the 3FGL sources within  $20^\circ$  from the cluster centroid, as well as the Galactic and extragalactic diffuse emission. A further source with a power-law spectral distribution was assumed at the MST coordinates. The normalization and spectral index of all the 3FGL sources within the ROI was allowed to vary in the fitting, while the parameters of the sources between  $10^\circ$  and  $30^\circ$  from the center of the field of view were fixed to their catalogue values. From this analysis, we derived the likelihood Test Statistics ( $TS$ ) and fluxes in the two 3–300 and 10–300 GeV bands. The results are reported in Table 2. Eight of the 19 MST clusters are significant from a likelihood analysis standpoint ( $TS > 25$ ) and therefore can be considered confirmed  $\gamma$ -ray sources; other six clusters have a  $TS$  value between 16 and 25, while only four have  $TS < 16$ . For MST 0848+0503 no significant result was obtained because of a confusion problem with another close blazar (see the discussion on Section 4.5). Fluxes above 3 and 10 GeV between a few  $10^{-10}$ – $10^{-11}$   $\text{ph cm}^{-2} \text{s}^{-1}$  are obtained for the safe sources whereas for those having a  $TS$  value below the conventional significance threshold ( $TS = 25$ , corresponding to  $5\sigma$ ) upper limits were computed. Note that three of the four clusters with the lowest significance have also low  $M$  values (15.81, 15.90, 17.95) while only MST 0801+6442 has a magnitude of 28.10, that is due to the relatively high number of photons in the cluster. This particular case will be discussed in more detail in Sect. 4.2.

<sup>4</sup><http://www.cv.nrao.edu/nvss/>

<sup>5</sup><http://sundog.stsci.edu/first/catalogs/readme.html>

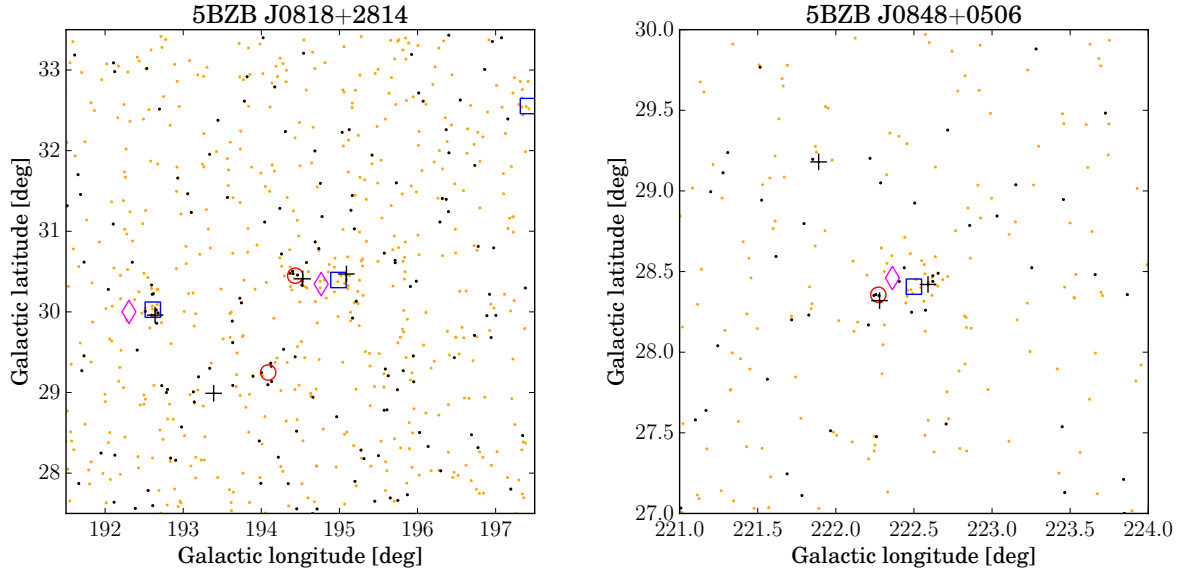


**Fig. 4**  $\gamma$ -ray sky maps in Galactic coordinates of the regions centered around the BL Lac objects 5BZB J0818+2814 (left panel) and 5BZB J0848+0506 (right panel), both having a rather close BL Lac object. Orange circles mark the photon coordinates at energies higher than 3 GeV and the black ones at energies higher than 10 GeV; black crosses corresponds to the optical coordinates of BL Lac objects in the 5BZCAT, blue open squares are the 3FGL sources, the open red circles are the MST cluster positions in the 10 GeV field, while the magenta diamonds are the positions of sources in the D<sup>3</sup>PO catalogue.

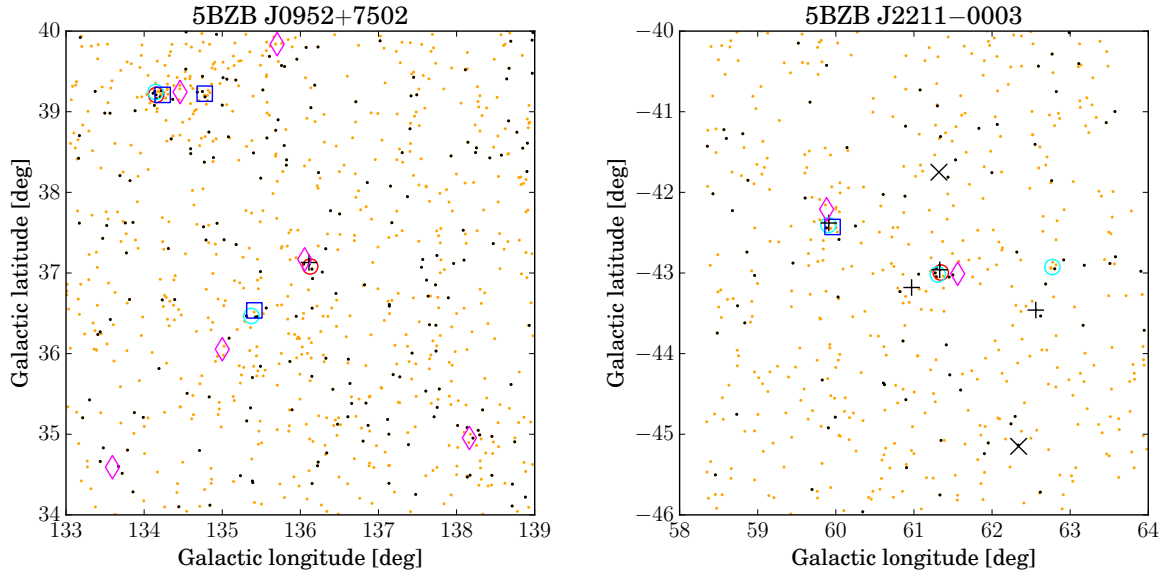


**Fig. 5** Photon sky maps in Galactic coordinates of the regions around the BL Lac objects 5BZB J0952+7502 (left panel) and BZB J2211-0003 (right panel). The longitude scale has been multiplied by the cosine of the mean latitude for a better imaging of angular distances. Orange circles mark the photon coordinates at energies higher than 3 GeV, magenta circles at energies higher than 6 GeV and the black ones at energies higher than 10 GeV; black crosses correspond to the optical coordinates of BL Lac objects in the 5Roma-BZCAT while black x-symbols are blazars of other type, blue open squares are the 3FGL sources, the open red circles are the MST cluster positions in the 10 GeV field and the open turquoise circle at energies above 3 GeV, while the magenta diamonds are the positions of sources in the D<sup>3</sup>PO catalogue.

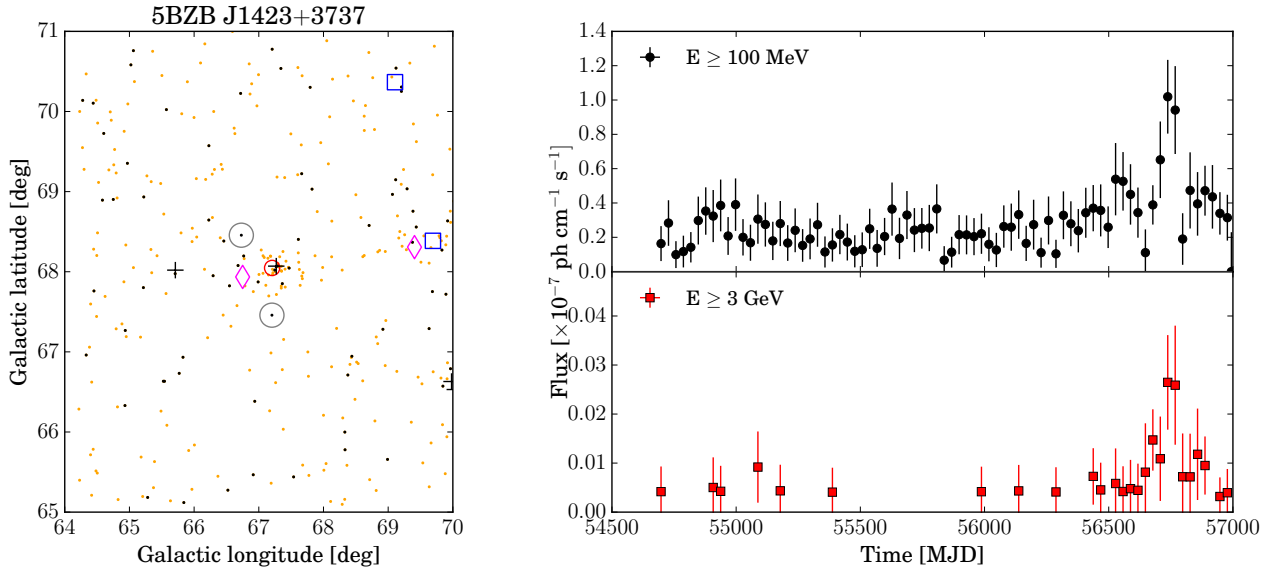


**Fig. 6** Photon sky map in Galactic coordinates of the region around the BL Lac objects 5BZB 1437+3737 (left panel), and aperture photometry light curve (right panel). The longitude scale has been multiplied by the cosine of the mean latitude for a better imaging of angular distances. Orange circles mark the photon coordinates at energies higher than 3 GeV, magenta circles at energies higher than 6 GeV and the black ones at energies higher than 10 GeV; black crosses correspond to the optical coordinates of BL Lac objects in the 5Roma-BZCAT while black x-symbols are blazars of other type, blue open squares are the 3FGL sources, the open red circles are the MST cluster positions in the 10 GeV field and the open turquoise circle at energies above 3 GeV, while the magenta diamonds are the positions of sources in the D<sup>3</sup>PO catalogue. The two grey circles indicate the locations of the two galaxy clusters A 1902 and A 1914.

#### 4 Comments on individual sources

Many of the newly associated BL Lac objects (10 over 19) have a value of  $\text{Log } \Phi_{\text{XR}}$  typical of HBL. SDSS DR10 photometric data are available for four of the other six sources with an LBL value and their  $u - r$  colours are smaller than 1.4, that according to Massaro et al. (2012) can be taken as the discriminating value between BL Lacs having a nucleus or galaxy dominated emission.

In the following we discuss in more detail some clustering properties of a few sources of the sample.

##### 4.1 5BZB J0204–3333

The association of the MST photon cluster MST 0204–3333 with 5BZB J0204–3333 should be considered not safely confirmed, since at a separation of 5' from the cluster centroid the rather bright flat spectrum radio source PKS J0204–3328 (AT20G J020428–332849) is present, for which an indication for a galaxy type counterpart of magnitude  $B = 23.1$  is reported (Titov and Malkin 2009). MST analysis in the same field at energies higher than 5 GeV gives a more conspicuous cluster ( $N = 10$ ,  $M = 31.9$ ) but fails to solve the positional ambiguity because photons are distributed around both sources.

##### 4.2 5BZB J0801+6444

As already noticed above the association of the cluster MST 080166442 with BZB J0801+6444 appears somewhat unsafe because the likelihood analysis gives a low  $\sqrt{TS} = 3.3$ , despite the high  $M$  value. A further analysis with the lower  $\Lambda_{\text{cut}} = 0.7$  reduces the number of photons in the cluster from 9 to 6 but increases the clustering factor  $g$  to 3.50 giving again a rather robust  $M = 20.99$ . Moreover, the centroid of the new cluster is at an angular separation from the possible counterpart of only 2'.4, reducing the chance association probability. This result could be an indication that the cluster can be affected by some photons of the local background that is reduced using a stronger cut length. MST search at energies higher than 3 GeV in a  $10^\circ \times 10^\circ$  region gives a more robust detection of a 15 photon cluster with  $M = 38.00$  and centroid coordinates at a very small separation (1'.3) from the BL Lac object.

##### 4.3 5BZB J0803+2440

This blazar and 5BZB J1352+5557 are associated with the two clusters having the lowest  $M$  values in the sample, but while the latter appears nearly validated by the ML analysis, the results on a possible  $\gamma$ -ray source close

**Table 2** Standard unbinned likelihood analysis of the *Fermi*-LAT data, see text for details. The last two columns report photon fluxes in units of  $10^{-11}$   $\text{ph cm}^{-2} \text{s}^{-1}$ . For sources below the usual significance threshold ( $TS = 25$ ) only upper limits are given.

MST cluster	$\sqrt{TS}$	Flux 3–300 GeV	Flux 10–300 GeV
MST 0204–3333	4.0	$\leq 6.7$	$\leq 1.0$
MST 0236–2940	4.6	$\leq 7.2$	$\leq 1.3$
MST 0336–0347	3.9	$\leq 5.5$	$\leq 1.4$
MST 0801+6442	3.3	$\leq 4.0$	$\leq 0.4$
MST 0803+2440	3.5	$\leq 4.1$	$\leq 0.8$
MST 0818+2819	5.0	$6.9 \pm 2.4$	$2.3 \pm 1.1$
MST 0848+0503	—	—	—
MST 0932+1042	5.4	$7.9 \pm 2.7$	$2.1 \pm 1.1$
MST 0947+2215	5.8	$9.5 \pm 2.9$	$2.2 \pm 1.1$
MST 0951+7503	4.6	$\leq 4.2$	$\leq 1.6$
MST 1005+6443	5.0	$6.3 \pm 2.1$	$1.5 \pm 0.8$
MST 1137–1706	6.7	$14.0 \pm 3.4$	$2.5 \pm 1.1$
MST 1216–0241	5.0	$6.4 \pm 2.5$	$2.4 \pm 1.2$
MST 1311+3951	2.9	$\leq 3.6$	$\leq 2.5$
MST 1352+5557	4.8	$\leq 7.9$	$\leq 4.8$
MST 1423+1414	4.4	$\leq 5.2$	$\leq 1.4$
MST 1423+3736	12.1	$22.8 \pm 3.7$	$4.3 \pm 1.5$
MST 1627+3148	7.0	$10.3 \pm 2.9$	$2.4 \pm 1.2$
MST 2211–0004	4.6	$\leq 7.6$	$\leq 1.6$

to 5BZB J0803+2440 give a rather poor significance (see Table 2). Nevertheless, there is some indication for a safer detection and a more robust association of the cluster with 5BZB J0803+2440. When selecting a smaller region of about  $5^\circ \times 5^\circ$  and applying a stronger cut with  $\Lambda_{\text{cut}} = 0.5$  in order to reduce possible the background contribution from distant photons we found above 10 GeV only two clusters (see Figure 3): one with 5 photons and  $M = 18.93$  nearly coincident with the previous one (RA = 120.760, DEC = 24.567) at the closer angular distance of  $1'.96$  from the blazar; and another cluster with only 4 photons and a lower clustering parameter ( $M = 13.92$ ) that corresponds to the 3FGL J0758.9+2705 source which is very close to the other blazar 5BZG J0758+2705. When considering energies higher than 3 GeV the latter cluster is much richer and has a very significant  $M = 60.9$ , while MST 0803+2440 is found with a very low  $M$  because it disappears in the stronger background. This could be an explanation of why at these energies ML results are poor. It is therefore possible that 5BZB J0803+2440 has a quite hard  $\gamma$ -ray spectrum that makes it detectable only at high energies and for this reason one can consider the association of the cluster with the BL Lac object as an interesting indication.

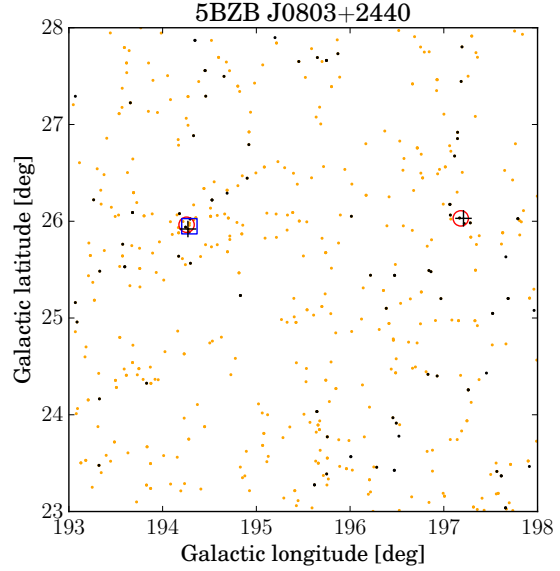


**Fig. 3**  $\gamma$ -ray sky maps in Galactic coordinates of the regions centered around the BL Lac objects 5BZB J0803+2440. Black circles mark the photon coordinates at energies higher than 10 GeV and orange ones above 3 GeV; black crosses corresponds to the optical coordinates of BL Lac objects in the 5BZCAT, blue open squares are the 3FGL sources, the open red circles are the MST cluster positions in the 10 GeV field.

#### 4.4 5BZB J0818+2814

This BL Lac object is located at angular distance of about  $29'$  to 5BZB J0819+2747, which is associated with the known  $\gamma$ -ray source 3FGL J0818.8+2751. The sky map in Figure 4 (left panel) clearly shows a photon cluster around 5BZB J0819+2747 at energies higher than 3 GeV. Photons above 10 GeV are densely located only around the position of 5BZB J0818+2814, while none is found close to the position of the other source. Consider also that the cluster has a quite high  $g$  and a corresponding median radius of about only  $4'$ , that corresponds to about 15% of the separation between sources. It appears, therefore, unlikely that photons in the MST cluster could be originated by a distant source without any concentration at the expected position.

A source at an intermediate position between our source and that of 3FGL J0818.8+2751 (see Figure 4) is also reported in the D<sup>3</sup>PO catalogue<sup>6</sup> (Selig et al. 2014), without indication of a possible counterpart.

<sup>6</sup>The Denoised, Deconvolved, and Decomposed Fermi  $\gamma$ -ray Sky, <http://www.mpa-garching.mpg.de/ift/fermi/>



#### 4.5 5BZB J0848+0506

A photon cluster is found at the angular separation of  $12'2$  from the gamma-ray source 3FGL J0849.3+0458, which is in the 2FGL and 2LAC catalogues and is reported as the counterpart to the BL Lac object 5BZB J0849+0455. This source is also in the D<sup>3</sup>PO catalogue, while there is no high-energy MST detection at these coordinates. However, at energies higher than 10 GeV, this angular separation between the centroid coordinates and the blazar results quite higher than the mean association distance (see Sect. 3 and Fig. 1) and therefore the connection between the cluster and the BL Lac object is rather weak. The cluster centroid is at a separation of  $5'5$  from another BL Lac object, 5BZB J0848+0506, that is not yet detected at  $\gamma$ -ray energies. The map in Figure 4 (right panel) illustrates this situation: a high concentration photon cluster is located very close to 5BZB J0848+0506 and not at the position of 5BZB J0849+0455. A significant cluster ( $M = 33$ ) is also found by MST at energies higher than 30 GeV, where the mean spatial density of photons in the region is very low. On the other hand, when repeating the MST analysis in the LAT field above 3 GeV we find a unique rich cluster with a very high MST magnitude ( $M = 88$ ) and very precisely located at the 5BZB J0849+0455 coordinates.

In these conditions it is hard to obtain a safe estimate the actual significance of the cluster MST 0848+0503 and its association with 5BZB J0848+0506 because there is no way to exclude photons from the other close bright BL Lac object that can accidentally be found in the MST cluster, the richest in the present sample. Note also that in Table 1 this BL Lac has the highest value of  $\text{Log } \Phi_{XR}$ , while no X-ray detection of 5BZB J0849+0455 is reported in the 5BZCAT. One can infer that the former source is a HBL object, and consequently with a particularly hard  $\gamma$ -ray spectrum, while the latter might be an LBL object with a possible high energy cut-off. In the 3FGL catalogue there are 14 sources associated with BL Lac objects with a radio flux density at 1.4 GHz lower than 10 mJy but detected in the X rays, as expected for HBL objects. Therefore, our association is not in contrast with previous results on  $\gamma$ -ray emission from this class of sources.

We can conclude, therefore, that both BL Lac objects are high energy emitters but their spectra are very different.

#### 4.6 5BZB J0952+7502

The sky map of the region around 5BZB J0952+7502 has a higher density of photons but a relative low number of  $\gamma$ -ray sources (Figure 5, left panel). There are

only two MST cluster detections above 10 GeV. The first corresponds to a 3FGL and D<sup>3</sup>PO source very close to the blazar 5BZU J1031+7441, while the second cluster is detected only at energies higher than 10 GeV. Excluding the farthest photon from the cluster, the new  $g$  and  $M$  are increased and also the positional matching improves, making stronger the association with this BL Lac object. Finally, the spectrum of this source must be rather peculiar with a possible turn off at low energies because it is undetected when energies higher than 3 GeV are considered.

#### 4.7 5BZB J1311+3953

The detection of the cluster MST 1311+3951 is rather critical because it presents three close photons surrounded by a few other photons which could be background events. A cluster of 7 photons is found at energies higher than 6 GeV in a  $10^\circ \times 10^\circ$  region, but with a rather low  $g$ , whereas there is no detection when a lower energy threshold of 3 GeV is considered. This explain the quite low  $\sqrt{TS} = 2.9$  value found from the ML analysis. It is interesting to note that the D<sup>3</sup>PO catalogue reports a source (1DF002707) with a photon flux of about  $5.0 \cdot 10^{-11}$  ph/(cm<sup>2</sup> s) and Galactic coordinates  $l = 105^\circ 811$ ,  $b = 76^\circ 446$ . The angular distance to the centroid of MST 1311+3951 is  $8'7$ , too large for a firm association, but small enough for suggesting a region with a possible extended emission or source confusion.

At energies higher than 10 GeV in a  $6^\circ$  size region MST analysis confirmed this cluster ( $M = 19.48$ ) and found only one very significant cluster at the position of 5BZB J1309+4305 (3FGL J1309.3+4304). In a wider  $10^\circ$  size region there are three other blazars listed in the Roma-BZCAT, two of them associated with 3FGL sources: 5BZB J1305+3855, 5BZQ J1308+3546 (3FGL J1308.7+3545) and 5BZB J1309+4305 (3FGL J1309.3+4304). We found at energies higher than 3 GeV again only one very significant cluster corresponding to the last one, in any case these blazars are well separated from MST 1311+3951 to produce any confusion.

We can conclude that there are some interesting indications for an high energy emission related to 5BZB J1311+3953, although it is quite difficult to obtain an entirely satisfactory statistical significance.

#### 4.8 5BZB J1423+3737

This source is the brightest in the sample and above 3 GeV its position correspond to a high density and rich cluster (Figure 6, left panel) In the same field there

are two 3FGL sources (3FGL J1411.1+3717 and 3FGL J1419.8+3819) at a separation higher than  $1^\circ$  and two D<sup>3</sup>PO sources, one of which corresponding to the latter object and the other close to 5BZG J1424+3705, but none of them associated with this BL Lac object. Note that this object was already reported as a possible counterpart to 3EG J1424+3734 in the Third EGRET catalogue (Hartman et al. 1999), although at a distance of about  $21'$ . It was also present in 1FGL and 1LAC (Abdo et al. 2010) catalogues, but disappeared in the subsequent versions. The EGRET source was also associated by Colafrancesco (2002) with the nearby galaxy clusters A 1902 and A 1914, whose locations are marked in the map of Figure 6 by two gray circles.

Two light curves of the events at energies above 0.1 and 3 GeV from a circular region of radius  $0.3^\circ$  centered at the source position (see Figure 6, right panel) were extracted. A flare in which the count rate increased by a factor of about 5, reaching  $>100$  MeV fluxes around  $10^{-7}$  photons  $\text{cm}^{-2} \text{s}^{-1}$  ( $\sim 3 \cdot 10^{-9}$  photons  $\text{cm}^{-2} \text{s}^{-1}$  above 3 GeV) and having a duration of  $\sim 3$  months is clearly apparent in the period from MJD 56550 to 56650 (2013 September–December), making more robust the identification of this 5BZB J1423+3737 as the counterpart to the  $\gamma$ -ray source. Moreover, this variability and the finding that no high energy photons are observed from the two near galaxy clusters seems to discount the possibility that these objects are powerful emitters of high energy  $\gamma$ -rays.

#### 4.9 5BZB J2211–0003

This is one of the most crowded field of blazars containing four BL Lac objects and two other type blazars (possibly FSRQ, Figure 5, right panel) There is only one 3FGL source which corresponds to the unique D<sup>3</sup>PO source and is associated with 5BZB J2206–0031. MST analysis above 3 GeV gives three significant clusters (open turquoise circles): one corresponding to this source, another related to a high concentration of a small number of photons at  $l = 62.77$ ,  $b = -49.93$ , and the third one very close to 5BZB J2211–0003. The last cluster is the only significant one found at energies higher than 10 GeV.

About the unassociated source we found an interesting possible radio counterpart, NVSS J223510–033332, at an angular separation of  $6.75'$  with a radio flux density at 1.4 GHz of 93 mJy. It corresponds in SDSS DR10 to a starlike object with  $r = 19.45$  mag and  $u-r = 0.90$ , typical of many HBL objects detected in the  $\gamma$ -ray band (Massaro et al. 2012).

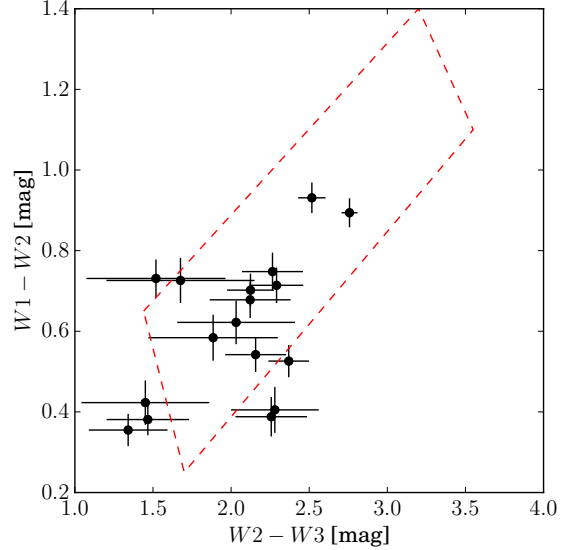


**Fig. 7** Plot of the infrared colours of the MST-selected BL Lac objects from the AllWISE catalogue. The dashed line define the region where the WISE Blazar strip is located according to the recent analysis by D’Abrusco et al. (2014). The majority of our sources lie within the strip and those outside the boundaries are generally affected by large errors making possible their location inside the  $\gamma$ -ray loud region.

## 5 Discussion

The new detections of  $\gamma$ -ray clusters closely associated with BL Lac objects at energies higher than 10 GeV confirm the high sensitivity of MST method in extracting small photon concentrations from a sparse background. This fact makes the method particularly able in detecting weak sources that, when observed at lower energies, could be confused with the background. We are confident that our detections are robust, not only for their high  $M$  values but also because the chance probabilities for such a good positional correspondence are indeed quite low. The two sources 5BZB J0801+6444 and 5BZB J1216–0243 are reported in the 5BZCAT as BL Lac candidates because their optical spectra are unpublished. Clearly our detection support their identification as genuine blazars.

We obtained also the significance of these clusters by evaluating their test statistics applying the standard LAT maximum likelihood method at energies higher than 3 GeV in ROI of  $10^\circ$  radius: for 14 clusters we obtained values of  $TS$  higher than 16 (8 of which with  $TS > 25$ ). For only 5BZB J0848+0506 we failed to obtain convergence because of the proximity of 5BZB J0849+0455. These results provide a practical validation of the minimal spanning tree clustering method to select candidate sources.

We also verified if the infrared colors of the reported BL Lac objects are compatible with the WISE blazar strip, discovered by Massaro et al. (2011, 2012) where the majority of  $\gamma$ -ray loud sources of this type are located. We obtained three band infrared photometric data from the AllWISE catalogue (Cutri and et al. 2014, data at  $22\ \mu\text{m}$  are available only for three sources) and computed the  $W1-W2$  and  $W2-W3$  colours without reddening correction because all the sources have a Galactic latitude higher than  $25^\circ$ . Figure 7 shows that the majority of these newly observed BL Lacs above 10 GeV are really aligned along the strip, whose approximate countour is marked by the red dashed line on the basis of the most recent plots given by D’Abrusco et al. (2014) (WIBRaLS catalogue). Sources outside the strip have photometric uncertainties large enough that they are also compatible generally within one standard deviation. Note, however, that only 5BZB 1437+3737 is reported in the WIBRaLS catalogue as class C object because it is one of the three sources detected in the  $22\ \mu\text{m}$  WISE bandpass.

We acknowledge use of archival Fermi data. We made large use of the online version of the Roma-BZCAT and of the scientific tools developed at the ASI Science Data Center (ASDC), of the Sloan Digital Sky Survey (SDSS) archive, of the NED database and other astronomical catalogues distributed in digital form (VizieR and Simbad) at Centre de Datas astronomiques de Strasbourg (CDS) at the Louis Pasteur University.

## References

- Abdo, A.A., Ackermann, M., Ajello, M., Allafort, A., Antolini, E., Atwood, W.B., Axelsson, M., Baldini, L., *et al.*: *Astrophys. J.* **715**, 429 (2010)
- Ajero, F., Ackermann, M., Ajello, M., Albert, A., Atwood, W.B., Axelsson, M., Baldini, L., Ballet, J., *et al.*: *Astrophys. J. Suppl. Ser.* **218**, 23 (2015)
- Ackermann, M., Ajello, M., Allafort, A., Asano, K., Atwood, W.B., Baldini, L., Ballet, J., Barbiellini, G., *et al.*: *Astrophys. J.* **765**, 54 (2013a)
- Ackermann, M., Ajello, M., Allafort, A., Atwood, W.B., Baldini, L., Ballet, J., Barbiellini, G., Bastieri, D., *et al.*: *Astrophys. J. Suppl. Ser.* **209**, 34 (2013b)
- Bernieri, E., Campana, R., Massaro, E., Paggi, A., Tramacere, A.: *Astron. Astrophys.* **551**, 5 (2013)
- Campana, R., Massaro, E., Gasparrini, D., Cutini, S., Tramacere, A.: *Mon. Not. R. Astron. Soc.* **383**, 1166 (2008)
- Campana, R., Bernieri, E., Massaro, E., Tinebra, F., Tosti, G.: *Astrophys. Space Sci.* **347**, 169 (2013)
- Colafrancesco, S.: *Astron. Astrophys.* **396**, 31 (2002)
- Cutri, R.M., *et al.*: *VizieR Online Data Catalog* **2328**, 0 (2014)
- D’Abrusco, R., Massaro, F., Paggi, A., Smith, H.A., Masetti, N., Landoni, M., Tosti, G.: *Astrophys. J. Suppl. Ser.* **215**, 14 (2014)
- Hartman, R.C., Bertsch, D.L., Bloom, S.D., Chen, A.W., Deines-Jones, P., Esposito, J.A., Fichtel, C.E., Friedlander, D.P., *et al.*: *Astrophys. J. Suppl. Ser.* **123**, 79 (1999)
- Massaro, E., Nesci, R., Piranomonte, S.: *Mon. Not. R. Astron. Soc.* **422**, 2322 (2012)
- Massaro, E., Maselli, A., Leto, C., *et al.*: *Multifrequency Catalogue of Blazars*, 5th edn. Aracne Editrice, Rome (2014)
- Massaro, E., Maselli, A., Leto, C., Marchegiani, P., Perri, M., Giommi, P., Piranomonte, S.: *Astrophys. Space Sci.* **357**, 75 (2015)
- Massaro, F., D’Abrusco, R., Ajello, M., Grindlay, J.E., Smith, H.A.: *Astrophys. J. Lett.* **740**, 48 (2011)
- Massaro, F., D’Abrusco, R., Tosti, G., Ajello, M., Gasparri, D., Grindlay, J.E., Smith, H.A.: *Astrophys. J.* **750**, 138 (2012)
- Neronov, A., Semikoz, D., Vovk, I.: *Astron. Astrophys.* **529**, 59 (2011)
- Nolan, P.L., Abdo, A.A., Ackermann, M., Ajello, M., Allafort, A., Antolini, E., Atwood, W.B., Axelsson, M., Baldini, L., Ballet, J., *et al.*: *Astrophys. J. Suppl. Ser.* **199**, 31 (2012)
- Selig, M., Vacca, V., Oppermann, N., Enßlin, T.A.: *ArXiv e-prints* (2014). 1410.4562
- Titov, O., Malkin, Z.: *Astron. Astrophys.* **506**, 1477 (2009). 0911.3221
- Tramacere, A., Vecchio, C.: *Astron. Astrophys.* **549**, 138 (2013)